J Mater Sci (2009) 44:5935–5938
DOI 10.1007/s10853-009-3744-9

LETTER

ME response of cofired trilayer magnetoelectric composites with partial texturing

Rashed Adnan Islam · Shashank Priya

Received: 25 June 2009 / Accepted: 15 July 2009 / Published online: 21 August 2009

Magnetoelectric (ME) effect is the combination of two types of materials property such as magnetostriction and piezoelectricity [1–3]. ME effect can be described as the induced electrical polarization under magnetic field or induced magnetization under electric field. The interrelation between ferroelectricity and magnetism allows the magnetic control of ferroelectric properties and vice versa [4–7]. The composite systems are easy to fabricate as compared to the single phase materials, cost effective, and have higher working temperature range [8–10]. Sintered composites fabricated by mixing of piezoelectric and ferromagnetic phases have been widely studied because of its simplicity in synthesis using well-established conventional ceramic processing technique. To enhance the ME coefficient of sintered composite, it is necessary to optimize the composition, microstructural features (grain size, grain orientation), geometry, and sintering parameters. In our previous studies, it have been shown that soft piezoelectric phase (high dielectric and piezoelectric constant), soft magnetic phase (high permeability and low coercivity) [11], large piezoelectric grain size (>1 μm) [12], layered structure (bilayer/trilayer) [13], and post-sintering thermal treatment (annealing and aging) [14] improve the ME property. For synthesizing the cofired trilayer composite, we introduced the noble pressure assisted sintering. We use this process to investigate the effect of grain texturing on ME coefficient of the trilayer composite.

Crystallographic texturing of piezoelectric phase can improve the piezoelectric and ferroelectric response by exploiting the anisotropy of electrical properties. Results have been reported in literature on the effect of texturing in both lead-based and lead-free materials including BTO, PMN-PT, NBT-BT, and KNN [15–18]. The goal of this study was to implement the known texturing process in heterogeneous system consisting of varying crystal structure. This will allow developing novel hybrid materials that exhibit maximum response. As a simple rule, the rhombohedral phase oriented along the $\langle 100 \rangle$ direction provides higher piezoelectric response. Texturing can be accomplished through various processes including, hot pressing (HP), templated grain growth (TGG) [19], and reactive template grain growth (RTGG) [15]. The advantage of TGG over HP is that the process is conducted using steps similar to that of conventional ceramic processing except with added seed material. In HP there is a chance of abnormal grain growth. Hence in this study, the TGG technique was adopted to synthesize the textured ME coefficient. The texturing process consists of two important steps (i) seed fabrication and (ii) seed alignment in the matrix [20].

To fabricate the seed (template), molten salt synthesis technique was utilized. In this respect, $BaTiO_3$ was chosen as the seed material since it can be grown in large size using Remeika process [21]. This synthesis process consists of heating the raw materials (BTO covered with KF salt in Pt crucible) in the temperature range of 1150–1225 °C (±5 °C) for 8–12 h and then slowly cooling down to the room temperature. The crystals were separated from

R. A. Islam (✉)
Materials Science and Engineering, University of Texas
at Arlington, Arlington, TX 76019, USA
e-mail: rashed_ms@yahoo.com

S. Priya
Materials Science and Engineering, Virginia Tech, Blacksburg,
VA 24061, USA

Present Address:
R. A. Islam
Sr. Materials Engineer, Eoplex Technologies Inc.,
Haven Avenue, Redwood City, CA 3698, USA

KF salt by hot water. The size of synthesized $BaTiO_3$ seed was found to be in the range of 75–200 µm. Some seeds were found to be as large as 2–3-mm plates. Figure 1a shows the optical image of the BTO seed fabricated using Remeika method showing facets at the surface, which could be related to the twins. A high magnification optical image (inset) shows these facets of single crystal cover the whole surface. X-ray diffraction pattern of the seeds in Fig. 1b shows strong intensity peak near 22.2°, which is the (001) peak of the perovskite BTO.

The seed crystals were used as templates for texturing piezoelectric phase in the trilayer ME composite. For this purpose, small amount (1–5 wt%) of seed was mixed with the piezoelectric powder $0.85Pb(Zr_{0.52}Ti_{0.48})O_3$–$0.15Pb(Zn_{1/3}Nb_{2/3})O_3$ (PZT–PZN). The seeded powder was mixed thoroughly and dried. Trilayer was pressed using ($Ni_{0.6}Cu_{0.2}Zn_{0.2}Fe_2O_4$) NCZF top and bottom layer with seeded PZT and 15% PZN in between. The sample was kept for sintering in an air atmosphere for 50-h soaking time so that the grains can grow along the preferred orientation of the seed crystal. A bilayer sample was also synthesized in order to study the structural characteristics of PZT layer. For each characterization, at least three samples from each batch were used and unless for identical results average values have been reported.

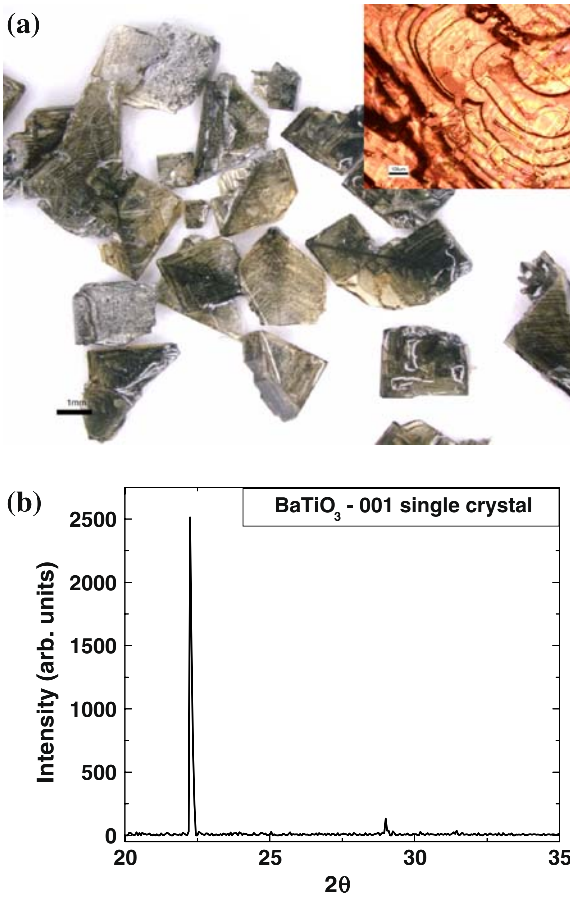

Fig. 1 **a** Optical images of large size BTO seed crystal (*inset*: facets or growth marks), **b** X-ray diffraction pattern of BTO seed showing (001) orientation

Figure 2 shows the X-ray diffraction pattern of the sample synthesized according to the above-mentioned procedure. The pattern shows considerable increase in (001)/(100), (111), (002)/(200) peak intensities compared to the (110)/(101) peak. Also the peak splitting is clearly observed in (001)/(100) and (002)/(220) peaks, which indicates the increase in tetragonality. From this pattern, the lattice parameter can be calculated to be $a = 4.008$ Å and $c = 4.098$ Å and the c/a ratio can be calculated as 1.022. Figure 2 also compares the XRD pattern of textured PZT–PZN with randomly oriented PZT–PZN. From X-ray diffraction patterns the degree of texturing was calculated by Lotgering method [20] as:

$$f_{00l} = \frac{P_{00l} - P_0}{1 - P_0}, \quad \text{where } P_{00l} = \frac{\sum I_{001}}{\sum I_{hkl}} \text{ and } P_0 = \frac{\sum I^0_{001}}{\sum I^0_{hkl}}$$

where I_{hkl} and I^0_{hkl} are the intensities of hkl plane for the textured and random sample, and $\sum I_{001}$ is the summation of the intensities of all 001 planes. Using this formula the Lotgering factor was calculated to be $f = 0.35$ for samples textured along ⟨001⟩ direction. Figure 3a shows the SEM microstructure of synthesized sample. Very large grains which are considered to be as textured grain with average size observed here is in the range of 200–350 µm compared to 1–2 µm size for randomly oriented grains. The grain size observed in Fig. 3a, b is very high due to large soaking period of 50 h, which also helps to orient the grains. Small-size seeds were observed near the textured grains. Figure 3c shows a completely randomly oriented

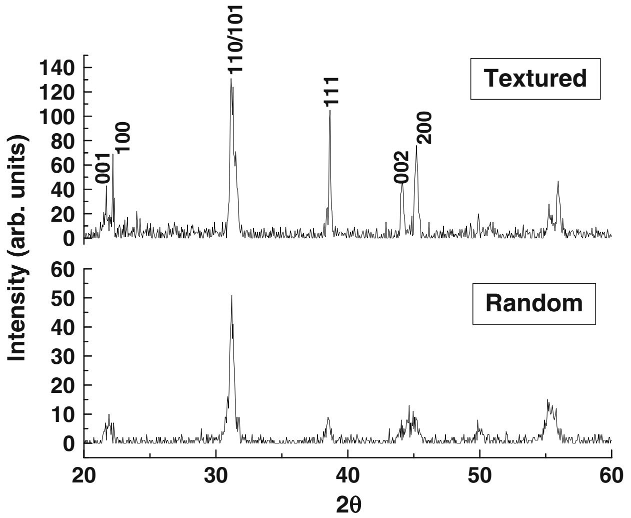

Fig. 2 X-ray diffraction pattern of textured PZT–PZN compared to randomly oriented PZT–PZN

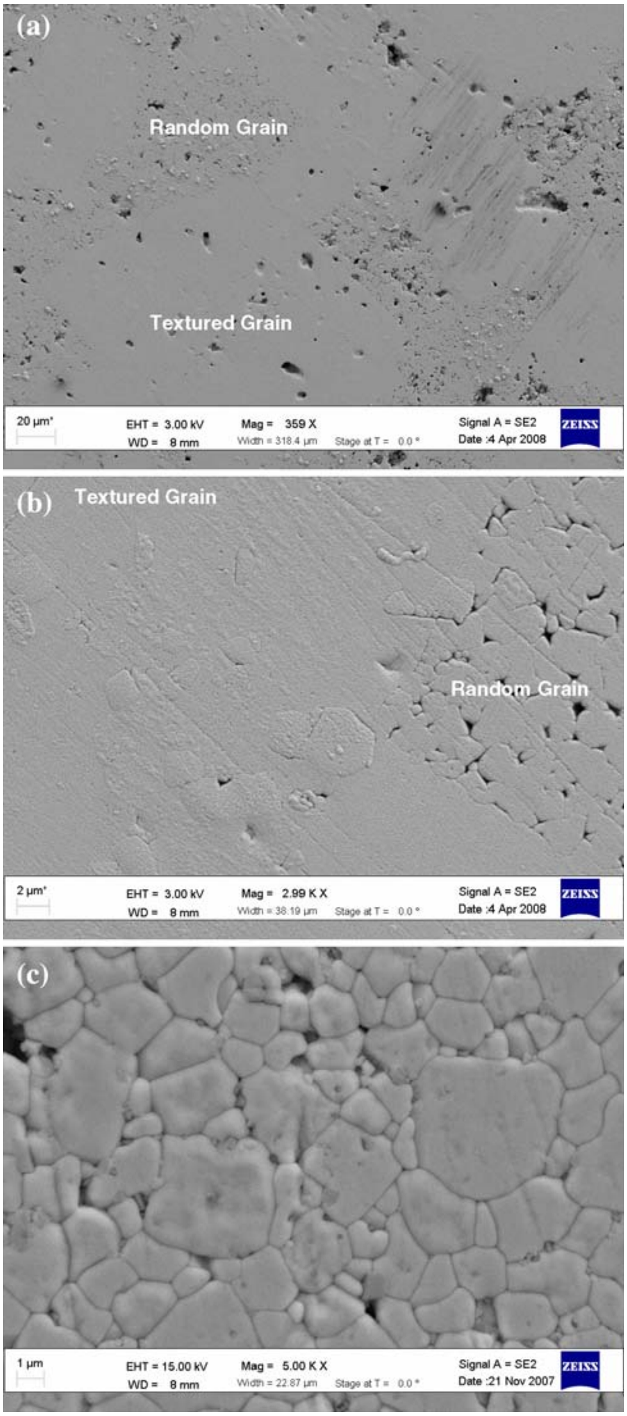

Fig. 3 **a** Low-magnification SEM micrographs of PZT–PZN with textured grains, **b** high-magnification SEM micrograph of PZT–PZN texture–random grain interface, and **c** high-magnification image of completely random PZT–PZN grains

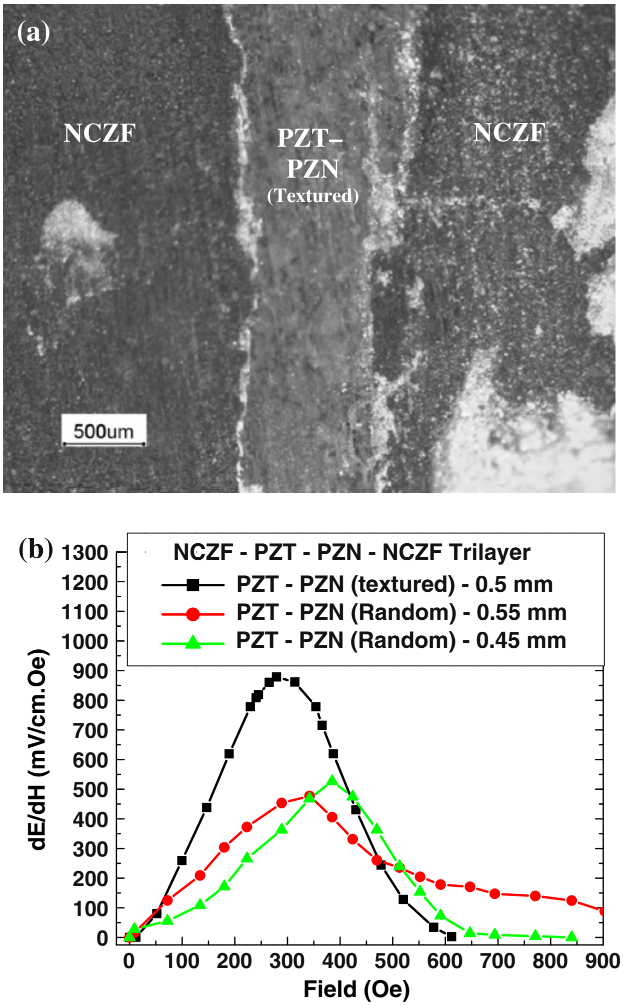

Fig. 4 **a** Optical images of NCZF–(textured PZT–PZN)–NCZF trilayer and **b** ME coefficient of this trilayer composite compared to random composite

PZT–PZN grains in the surrounding matrix with average grain size of greater than 1 μm grain size. These are preliminary results related to texturing and more in depth study is required to confirm the orientation and the degree of texturing. Figure 4a shows the optical images of cross-section of the trilayer which was poled for piezoelectric and ME characterizations. The cross-section shows crack-free interfaces with intact electrode layer. PZT–PZN layer was found to be around 0.5 ± 0.02 mm in thickness and NCZF thickness was of the order of 1.2 ± 0.05 mm. The samples were pooled at 120 °C for 20 min under a field of 2.5 kV/mm in a silicone oil bath. The longitudinal piezoelectric constant (d_{33}) was measured to be 325 ± 10 pC/N with dielectric constant of 1865 ± 30 and loss of 0.7% at room temperature measured at 1 kHz. Compared to the random PZT–PZN intermediate layer, d_{33} increases by ~44% and dielectric constant increases by ~50% for the moderate degree of texturing. Figure 4b shows the average ME coefficient of trilayer with textured PZT–PZN as a function of DC bias. Three samples from each batch were measured and the average value has been reported. The deviation observed from sample to sample within each batch is around 5%. The peak ME coefficient observed was around 878 ± 20 mV/cm Oe at 300 Oe DC bias field. For randomly oriented PZT–PZN layers, ME coefficient observed was around 526 ± 25 mV/cm Oe for 0.45-mm thickness of PZT–PZN and around 500 ± 15 mV/cm Oe for 0.55-mm. This increase in piezoelectric and ME coefficient in the textured trilayer can be explained in terms of domain engineering.

In summary moderately textured piezoelectric phase of [PZT–PZN] was synthesized in the trilayer ME composite to observe the effect of grain orientation. It was found that the trilayer composite shows improved piezoelectric and dielectric constant with enormous development in ME response. ME coefficient of 878 ± 20 mV/cm Oe was recorded which is almost 67% enhancement in magnitude compared to the trilayer with randomly oriented PZT–PZN phase. From these results a giant ME coefficient in sintered composite can realized by orienting the piezoelectric grains.

Acknowledgement This research was sponsored by Army Research Office.

References

1. Ryu J, Carazo AV, Uchino K, Kim H (2001) J Electoceram 7:17
2. Feibig M (2005) J Phys D 38:R123
3. Lupeiko TG, Lisnevskaya IV, Chkheidze MD, Zvyagintsev BI (1995) Inorg Mater 31:1139
4. Wang J, Zheng H, Lofland SE, Ma Z, Ardabili LM, Zhao T, Riba LS, Shinde SR, Ogale SB, Bai F, Viehland D, Jia Y, Schlom DG, Wuttig M, Roytburd A, Ramesh R (2004) Science 303:661
5. Ederer C, Spaldin N (2004) Nat Mater 3:849
6. Eerenstein W, Mathur ND, Scott JF (2006) Nature 442:759
7. Hur N, Park S, Sharma PA, Ahn JS, Guha S, Cheong S-W (2004) Nature 429, 392
8. Zheng M, Wan JG, Wang Y, Yu H, Liu JM, Jiang XP, Nan CW (2004) J Appl Phys 95(12):8069
9. Zhai J, Xing Z, Dong S, Li J, Viehland D (2008) J Am Ceram Soc 91(2):351
10. Flores VC, Baques DB, Flores DC, Aquino JAM (2006) J Appl Phys 99:08J503
11. Islam RA, Viehland D, Priya S (2008) J Mater Sci Lett 43(4):1497
12. Islam RA, Priya S (2008) J Mater Sci 43(10):3560. doi:10.1007/s10853-008-2562-9
13. Islam RA, Priya S (2006) J Appl Phys Lett 89:152911
14. Islam RA, Jiang JC, Priya S, Bai F, Viehland D (2007) Appl Phys Lett 91:162905
15. Takeuchi T, Tani T, Saito Y (1999) Jpn J Appl Phys 38:5553
16. Hong SH, Mckinstry ST, Messing G (2000) J Am Ceram Soc 83(1):113
17. Moure A, Pardo L, Alemany C, Millan P, Castro A (2001) J Eur Ceram Soc 21:1399
18. Allahverdi M, Hall A, Brennan R, Ebrahimi ME, Hagh NM, Safari A (2002) J Electroceram 8:129
19. Watari K, Brahmaroutu B, Messing G, Mckinstry S, Cheng SC (2000) J Mater Res 15(4):846
20. Sabolsky E, Mckinstry S, Messing G (2003) J Appl Phys 93(7):4072
21. Remeika JP (1953) Notes 76:940